2P4-4

Proceedings of Symposium on Ultrasonic Electronics, Vol. 34 (2013) pp. 269-270
20-22 November, 2013

Piezoelectric Vibration Energy Harvesters with Distinct Electrode Arrangements

Yung-Yu Chen† and Hua-Wen Pan
Department of Mechanical Engineering, Tatung University, Taiwan

1. Introduction

Piezoelectric vibration energy harvesters are attractive as inexhaustible power supply for low-power wireless electronic systems, particularly the tire pressure monitoring system (TPMS) [1-6]. The TPMS can indicate the slow leaks and warns the driver in time before the tire risks irreversible damage. In this paper, piezoelectric harvesters for gathering the vibration energy of cars running on rough ground are developed to substitute the battery in TPMS for advantage of being maintenance-free. Commercial finite element software, COMSOL multiphysics, was utilized to calculate output power of the piezoelectric energy-harvesting devices (EHDs) with taking load resistances into account. Three kinds of piezoelectric EHDs, like d_{31} unimorph, d_{31} bimorph, and d_{33} unimorph, were analyzed and designed for TPMS.

2. Results

2.1 The CPC-FEM model

A variety of modeling approaches [7-14] have been used to analyze the outputs of piezoelectric EHD, like uncoupled analyses, equivalent electric circuit methods, advanced modeling methods, and coupled piezoelectric-circuit finite element model (CPC-FEM). In this study, commercial finite element software, COMSOL multiphysics, was used to develop the CPC numerical model of a piezoelectric EHD connected directly with a load resistor. As shown in **Fig. 1**, three kinds of piezoelectric EHDs, including d_{31} unimorph, d_{31} bimorph, and d_{33} unimorph, are considered in the simulation. The EHDs are piezoelectric sandwich structures with a central brass substrate layer and one or two piezoelectric material layers. Their dimensions are listed in **Table 1**. The piezoelectric material was chosen to be the default PZT-5A in COMSOL. The electrode thickness is ignored in all simulations. The vibration amplitude and quality (Q) of the piezoelectric plate were set to be 25 μm and 65, respectively. Special focus is taken on the effect of load resistance on output power as well as the influences of the EHD's dimensions on resonance frequency and output power.

yychen@ttu.edu.tw

2.2 Simulation results

Figure 2 shows the open circuit voltages of the d_{31} unimorph and d_{33} unimorph. Since the piezoelectric coefficient d_{33} is two times larger than d_{31} in the PZT-5A layer, the d_{33} unimorph shows an output voltage of two times larger than the d_{31} unimorph. This result is also obtained from analytical method [15].

In a d_{31} bimorph, two piezoelectric layers can be connected to a load resistor by parallel or series connection. In the series connection, the polarizations of the two piezoelectric layers are opposite; in the parallel connection, the polarizations are identical. **Figure 3(a)** is the root mean square voltage versus load resistance for the d_{31} bimorph. When the load resistance increases, the voltage increases and the current decreases. **Figure 3(b)** shows the simulated output power versus load resistance. A maximal output power occurs at an optimal resistance. One can see that the optimal resistance in series configuration is 4 times higher than parallel configuration; the root mean square voltage of series configuration is 2 times higher than parallel configuration, but the current is only half of parallel configuration. Therefore, the output powers of both configurations are the same.

Figure 4 shows output power versus load resistance for the three EHDs. The d_{31} bimorph has a larger output power, and all the output powers are enough to power the wireless tire pressure monitoring system when the vibration amplitude is 25 μm. Moreover, when connecting to a load of lower resistance, the output power of d_{31} unimorph is higher than d_{33} unimorph; however, if connecting a load of higher resistance, the output power of d_{33} unimorph is higher than d_{31} unimorph.

3. Conclusions

The piezoelectric EHDs with distinct electrode arrangements were analyzing and designing for gathering the vibration energy of cars running on rough ground to substitute the battery in TPMS. The finite element software was utilized to calculate output power with taking load resistor into account. Results show that when the external resistance is 500 kΩ, the EHD of d_{31} unimorph yields a output power of 1.5 mW. Such output power is enough to power the wireless tire pressure monitoring system. The results of this paper can provide important guidelines for designing piezoelectric vibration

energy harvesters integrated with a wireless sensor system as well as the TPMS.

Acknowledgment
The authors gratefully acknowledge the financial support from National Science Council of Taiwan under the grant NSC 102-2221-E-036-008 and Tatung University in Taiwan through the grant B99-M06-006.

References

1. C. Shearwood and R.B. Yates: Electron. Lett. 33 (1997) 1883.
2. R. Amirtharajah and A.P. Chandrakasan: IEEE J. Solid-State Circ. 33 (1998) 687.
3. S. Meninger, J.O. Mur-Miranda, R. Amirtharajah, A.P. Chandrakasan, and J.H. Lang: IEEE T. VlSI Syst. 9 (2001) 64.
4. N.M. White, P. Glynne-Jones, and S.P. Beeby: Smart Mater. Struct. 10 (2001) 850.
5. C.T. Pan and T.T. Wu: J. Micromech. Microeng. 17 (2007) 120.
6. S.-J. Jeong, M.-S. Kim, J.-S. Song, and H.-K. Lee: Sens. Actuat. A 148 (2008) 158.
7. G.K. Ottman, H. F. Hofmann, and G. A. Lesieutre: IEEE Trans. Power Electron. 18 (2003) 696.
8. F. Lu, H.P. Lee, and S.P. Lim: Smart Mater. Struct. 13 (2004) 57.
9. S. Roundy, E.S. Leland, J. Baker, E. Carleton, E. Reilly, E. Lai, B.Otis, J.M. Rabaey, P.K. Wright, and V. Sundararajan: IEEE Trans. Pervasive Comput. 4 (2005) 28.
10. E. Lefeuvre, A. Badel, C. Richard, and D. Guyomar: J. Intell. Mater. Sys. Struct. 16 (2005) 865.
11. D. Guyomar, A. Badel, E. Lefeuvre, and C. Richard: IEEE Trans. Ultrason. Ferroelectr. Freq. Control 52 (2005) 584.
12. C. Shu and I.C. Lien: Smart Mater. Struct. 15, (2006) 1499.
13. E. Lefeuvre, A. Badel, C. Richard, L. Petit, and D. Guyomar: Sens. Actuators A 126 (2006) 405.
14. M. Zhu, E. Worthington, and J. Njuguna: IEEE Trans. Ultrason. Ferroelectr. Freq. Control 56 (2009) 1309.
15. R. Sood, Y.B. Jeon, J.H. Jeong, and S.G. Kim: Proceeding of Solid-State Sensor and Actuator Workshop (2004) 148.

Table 1 Dimensions of energy-harvesting devices

Components \ Dimensions	Length (mm)	Width (mm)	Thickness (mm)
Stainless steel	55.4	15.2	0.2
PZT-KA2	25.4	15.2	0.35
Mass	20	15.2	1.2

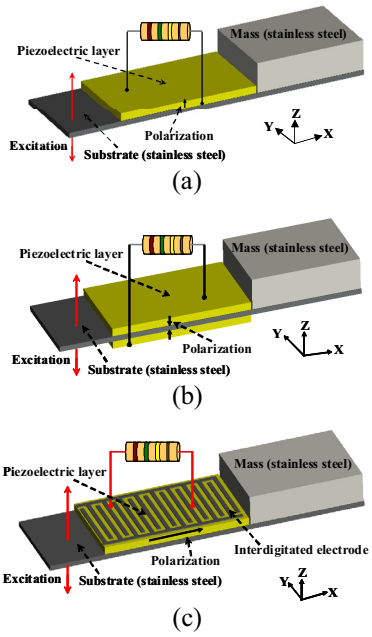

Fig. 1 Schematics of energy-harvesting devices: (a) d_{31} unimorph, (b) d_{31} bimorph, and (c) d_{33} unimorph.

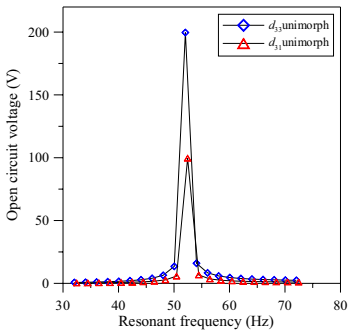

Fig. 2 Open circuit voltages of the d_{31} unimorph and d_{33} unimorph.

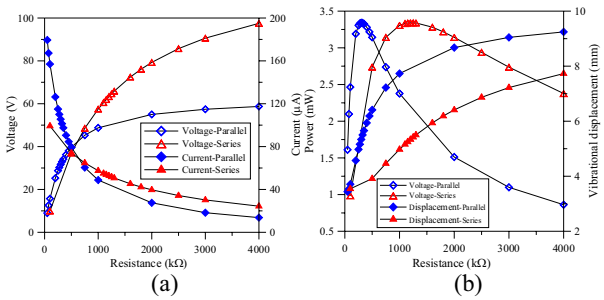

Fig. 3 (a) Voltage and (b) output power of the d_{31} bimorph in parallel and series connections.

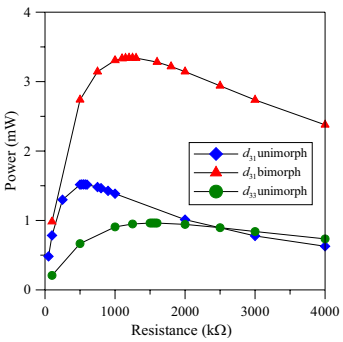

Fig. 4 Output power of energy-harvesting devices